Journal of Structural Geology, Vol. 5, No. 3/4, pp. 369 to 381, 1983
Printed in Great Britain

0191-8141/83 $3.00 + 0.00
Pergamon Press Ltd.

Theoretical strain patterns in ductile zones simultaneously undergoing heterogeneous simple shear and bulk shortening

J. INGLES

Laboratoire de Tectonophysique, Université Paul Sabatier, IUT, Département de Génie Civil, 50A, Chemin des Maraîchers, 31062, Toulouse Cedex, France

(*Received* 28 *June* 1982; *accepted in revised form* 18 *January* 1983)

Abstract—Structures observed in ductile shear zones show that deformation is continuous and strain is heterogeneous. This leads us to define a simple model for shear strain rate $\dot{\gamma}$. When a shear zone simultaneously undergoes simple shearing and pure shearing (contraction or extension), the condition of continuity of deformation shows that $\dot{\gamma}$ must be a function of time.

Integration of the deformation-rate equations yields the particle paths in the deforming body. From these we can determine, at any time and at any point in the body, the finite strain tensor (lengths and orientations of the axes of the finite strain ellipsoid); we can therefore define the finite strain trajectories and compare them with orientations of internal structures (schistosity, tension gashes).

The particle paths also allow us to study the progressive deformation of passive strain markers.

INTRODUCTION

STUDIES of finite strain in ductile zones that have undergone simple shear show that deformation is continuous in space and strain is heterogeneous (Ramsay 1967, Ramsay & Graham 1970, Hara *et al.* 1973); for example Fig. 1 shows a shear zone where the finite amount of simple shear γ changes continuously, and the induced schistosity takes a sigmoidal form.

However, simple shear alone cannot be responsible for the development of structures where the schistosity is continuous in and out of the shear zone (Fig. 2) (Ramsay & Graham 1970, Coward 1976, Cobbold 1977). Such structures can result from superposition of pure shear and heterogeneous simple shear during the same event of deformation. This combination is generally enough to describe most kinds of strain that rocks may undergo (Ramsay 1979).

Integration of the rate-of-deformation equations yields an equation which describes the path of any particle in the deforming body (Ramberg 1975). This equation can be used to determine the finite strain tensor (lengths and orientations of the axes of the finite strain ellipsoid) at any time and at any point of the body. We can therefore define finite-strain trajectories and compare them with oriented internal structures related to the direction and intensity of principal strains. In ductile zones, schistosity develops approximately normal to the short axis of the finite strain ellipsoid (Ramsay 1967, Elliott 1972, Gray & Durney 1979). In brittle-ductile zones, tension gashes form perpendicular to the large axis of the finite strain ellipsoid (Ramsay 1967, Jaeger 1969).

The particle-path equation also allows us to study the progressive deformation of passive strain markers with the same rheological properties as the surrounding material.

MODEL

We study plane strain of a continuous, homogeneous, incompressible and initially isotropic material subject to a steady uniform pure shear with axes x y (the principal strain rates $\dot{e}_x$ and $\dot{e}_y$ being constant both in the plane and

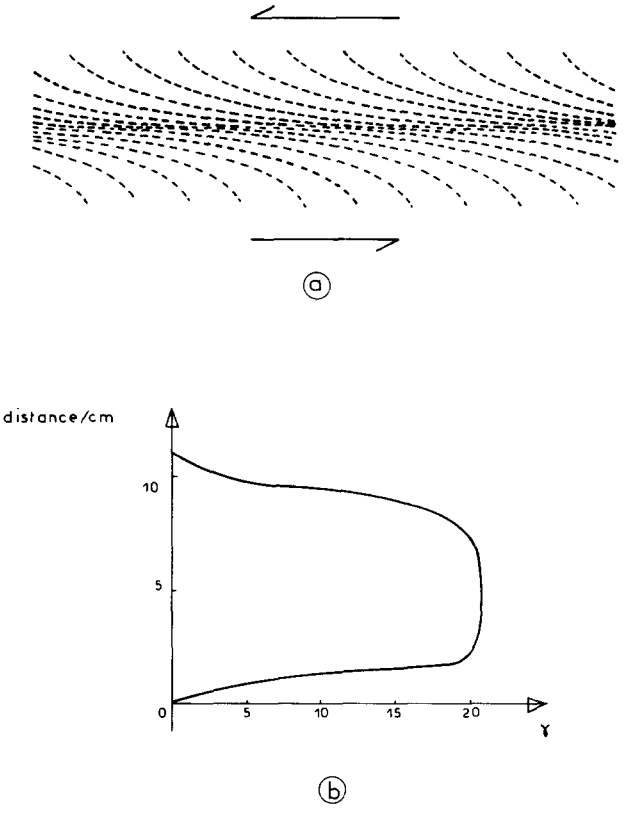

Fig. 1. Ductile shear zone in Lewisian metagabbro, Castell Odair, N. Uist, Scotland (after Ramsay & Graham 1970). (a) Sigmoidal shape of schistosity. (b) Variation of γ as deduced from orientation of schistosity, assuming simple shear.

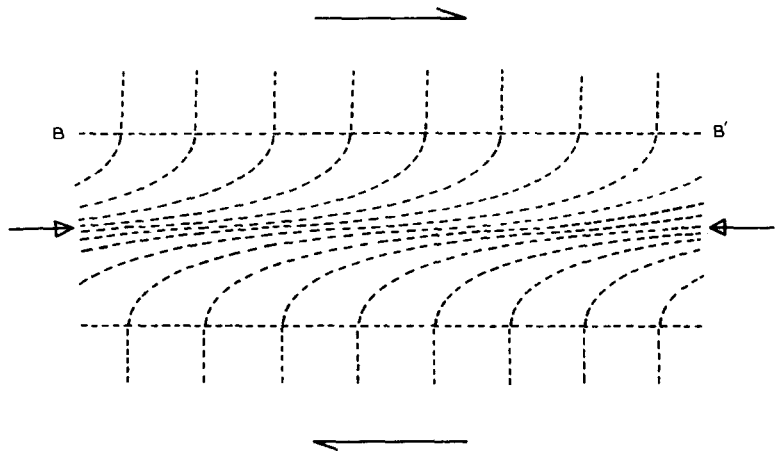

Fig. 2. Pattern of schistosity passing continuously across a ductile shear zone; granite from Cristallina, Ticino, Central Switzerland (after Ramsay & Graham 1970); (B.B'. = boundary of shear zone).

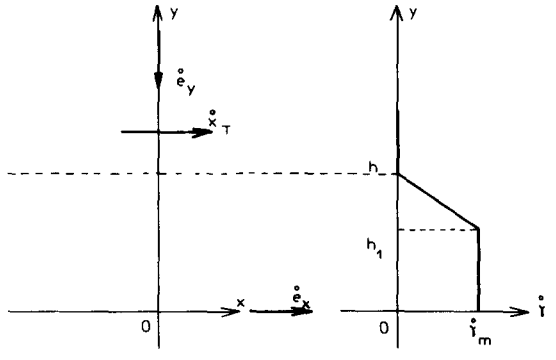

Fig. 3. Model of variation of $\dot{\gamma}$ throughout a ductile shear zone.

in time), in which a heterogeneous simple shear zone functions simultaneously. The direction of simple shear is parallel to the x axis; the shear zone is symmetrical relative to the x axis.

In order to represent, at time t, the variation of the rate of shear strain $\dot{\gamma}$ throughout the shear zone, we use a simple model of trapezoidal form (Fig. 3). In a central zone the deformation is homogeneous. Outside this, $\dot{\gamma}$ decreases in a linear fashion and vanishes at the limit of the shear zone. Thus

$$\begin{aligned} &\dot{\gamma} = \dot{\gamma}_m && \text{for } 0 \leqslant y \leqslant h_1, \\ &&& \text{homogeneous shear zone} \\ &\dot{\gamma} = \frac{\dot{\gamma}_m}{h - h_1}(h - y) && \text{for } h_1 \leqslant y \leqslant h, \\ &&& \text{heterogeneous shear zone} \\ &\dot{\gamma} = 0 && \text{for } y \geqslant h, \\ &&& \text{non-sheared zone.} \end{aligned} \tag{1}$$

Therefore the shearing is heterogeneous in space, but steady in time.

Half the initial thickness h_0 of the shear zone is taken as the unit of length ($h_0 = 1$); its value is h at time t. The initial half-thickness, h_{01}, of the central part of the shear zone, where the deformation is homogeneous, becomes h_1 at time t. The rates of displacement are expressed as units of length per unit of time and the rate of deformation in unit^{-1} of time. $\dot{e}_x$ is constant in the three zones: if $\dot{e}_x < 0$, the zones are extended, and if $\dot{e}_x > 0$, the zones are contracted. $\dot{e}_x = 0$ corresponds to a simple shear zone without bulk shortening/extension.

This model agrees well with observations made in natural ductile shear zones (Fig. 1). A linear variation of $\dot{\gamma}$ exists also, for example, in the heterogeneous shear zone appearing at the contact with the walls during the flow of a visco-plastic fluid in a pipe (Reiner 1960).

PARTICLE PATHS

The particle paths and streamlines are obtained by integrating the velocity at any point in the deforming body. For pure shear of an incompressible material undergoing plane strain, $\dot{e}_y = -\dot{e}_x$ so the velocity is

$$\begin{pmatrix} \dot{x}_e \\ \dot{y}_e \end{pmatrix} = \begin{pmatrix} \dot{e}_x & 0 \\ 0 & -\dot{e}_x \end{pmatrix} \begin{pmatrix} x \\ y \end{pmatrix}. \tag{2}$$

(The subscript e indicates that this displacement is due to pure shear alone).

For simple shear, the rate of shear strain $\dot{\gamma}$ is the gradient of the velocity parallel to the shear direction.

$$\dot{\gamma} = \frac{d\dot{x}_\gamma}{dy},$$

from which $d\dot{x}_\gamma = \dot{\gamma}\,dy$, so that the velocity at a distance y from the x axis is

$$\begin{aligned} \dot{x}_\gamma &= \int_0^y \dot{\gamma}\,dy, \\ \dot{y}_\gamma &= 0. \end{aligned} \tag{3}$$

(The subscript γ indicates that the displacement is due to simple shear alone.)

When the two kinds of motion occur simultaneously, the velocity at any point (x, y) is obtained by addition of (2) and (3)

$$\dot{x} = \dot{e}_x x + \int_0^y \dot{\gamma}\,dy, \qquad \dot{y} = -\dot{e}_x y. \tag{4}$$

The velocity component parallel to the y axis is that of pure shear alone:

$$\dot{y} = \frac{dy}{dt} = -\dot{e}_x y,$$

from which

$$\frac{dy}{y} = -\dot{e}_x\,dt.$$

By integration we obtain

$$y = y_0 \exp(-\dot{e}_x t),$$

where y_0 is the initial ordinate of the point considered. From this equation, we find the value at time t of h_0,

$$h = h_0 \exp(-\dot{e}_x t) = \exp(-\dot{e}_x t),$$

and that of h_{01},

$$h_1 = h_{01} \exp(-\dot{e}_x t).$$

When pure shear and simple shear occur simultaneously, the value of $\dot{x}_\gamma$ is obtained by integration of (3), where $\dot{\gamma}$ is a function of y, h and h_1, given by (1):

$$\dot{x}_\gamma = \dot{\gamma}_m y = \dot{\gamma}_m y_0 \exp(-\dot{e}_x t) \quad \text{for } 0 \leq y \leq h_1,$$

$$\dot{x}_\gamma = \dot{\gamma}_m \frac{-y^2 + 2hy - h_1^2}{2(h - h_1)} = \dot{\gamma}_m \frac{-y_0^2 + 2y_0 - h_{01}^2}{2(1 - h_{01})} \exp(-\dot{e}_x t) \quad \text{for } h_1 \leq y \leq h,$$

$$\dot{x}_\gamma = \dot{\gamma}_m \frac{h + h_1}{2} = \dot{\gamma}_m \frac{1 + h_{01}}{2} \exp(-\dot{e}_x t) \quad \text{for } y \geq h.$$

The equation for $\dot{x}_\gamma$ can therefore be written in the general form

$$\dot{x}_\gamma = \dot{\gamma}_m f(y_0) \exp(-\dot{e}_x t), \tag{5}$$

where $f(y_0) = y_0$ for $0 \leq y \leq h_1$,
$f(y_0) = ay_0^2 + by_0 + c$ for $h_1 \leq y \leq h$,
$f(y_0) = k$ for $y \geq h$.

Continuity of deformation at the boundary of the shear zone leads to an identity between $\dot{x}_\gamma$ and the rate of translation $\dot{x}_T$ of the non-sheared zone:

$$\dot{x}_T = k\dot{\gamma}_m \exp(-\dot{e}_x t).$$

In general, the translation of the non-sheared material is subordinate to kinematic conditions outside the shear zone and $\dot{x}_T$ is a function of time. The rate of shear strain,

$$\dot{\gamma}_m = [\dot{x}_T \exp(\dot{e}_x t)]/k \tag{6}$$

is thus a function of time.

The hypothesis that $\dot{\gamma}$ and $\dot{\gamma}_m$ remain constant during deformation (Ramberg 1975) is probably not realistic because it implies that $\dot{x}_T$ is a perfectly well-defined function of time and of $\dot{e}_x$,

$$\dot{x}_T = A \exp(-\dot{e}_x t).$$

Knowledge of $\dot{x}_T$ allows us to determine, by integrating (4), the equation of the particle path; if $\dot{x}_T$ is constant, $\dot{\gamma}$ is a function of time t and of the ordinate y of the point defined by (1) and (6).

Equation (4) gives

$$\dot{x} = \frac{dx}{dt} = \dot{e}_x x + \dot{\gamma}_m f(y_0) \exp(-\dot{e}_x t).$$

Introducing $\dot{\gamma}_m$ from (6),

$$\frac{dx}{dt} = \dot{e}_x x + \frac{\dot{x}_T}{k} f(y_0).$$

Integration yields the equation of the particle path:

$$x = x_0 \exp(\dot{e}_x t) + \frac{\dot{x}_T}{k\dot{e}_x} f(y_0)[\exp(\dot{e}_x t) - 1], \qquad y = y_0 \exp(-\dot{e}_x t) \tag{7}$$

where (x_0, y_0) are the initial coordinates of the point considered.

FINITE STRAIN

From the equation of the particle path, (7), we can determine the tensor of deformation gradients,

$$\begin{pmatrix} \frac{\partial x}{\partial x_0} & \frac{\partial x}{\partial y_0} \\ \frac{\partial y}{\partial x_0} & \frac{\partial y}{\partial y_0} \end{pmatrix} \equiv \begin{pmatrix} A & B \\ C & E \end{pmatrix}.$$

In the case studied here, $C = 0$ so the principal finite strains (lengths of the semi-axes of the strain ellipse $(\lambda_1)^{1/2}$ and $(\lambda_2)^{1/2}$, Fig. 4), are given by (Nadai 1950)

$$\lambda_{1,2} = \frac{1}{2(AE)^2}\,[A^2 + B^2 + E^2 \pm [(A^2 + B^2 - E^2)^2 + 4(BE)^2]^{1/2}]. \tag{8}$$

The principal directions of strain (Fig. 4) are given by

$$\tan \Phi_M = \frac{E^2 - \lambda_2(AE)^2}{BE} \tag{9a}$$

$$\tan \Phi_m = \frac{E^2 - \lambda_1(AE)^2}{BE}. \tag{9b}$$

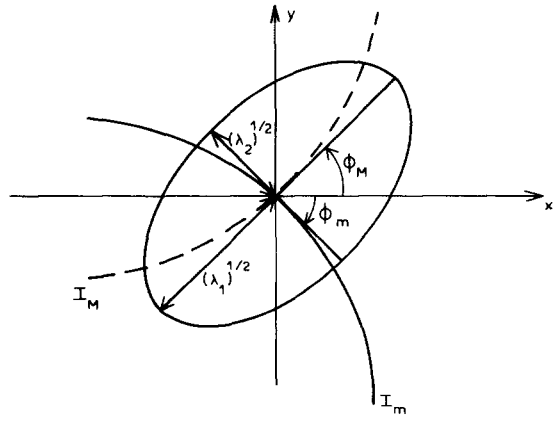

Fig. 4. Finite strain ellipse and finite strain trajectories, I_m, I_M, in a shear zone.

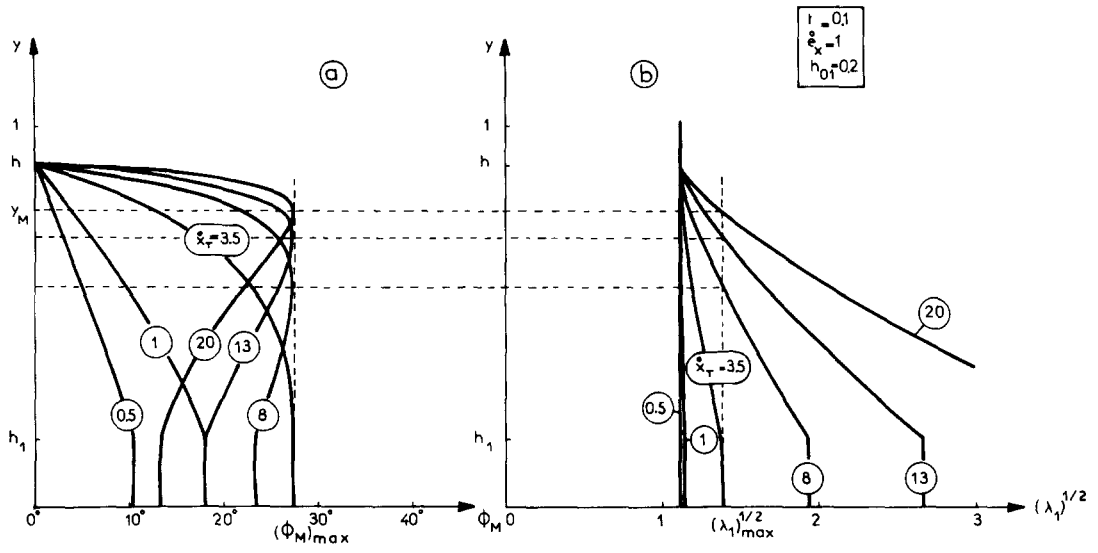

Fig. 5. Variation of (a) Φ_M and (b) $\lambda_1^{1/2}$ throughout the shear zone, for several values of $\dot{x}_T$ numbered.

We can thus determine the finite strain trajectories, I_M and I_m. I_M, which is the integral curve of

$$\frac{dy}{dx} = \tan \Phi_M, \tag{10a}$$

is perpendicular at every point to the minor principal strain, λ_2 (Fig. 4); I_m, which is the integral curve of

$$\frac{dy}{dx} = \tan \Phi_m, \tag{10b}$$

is perpendicular at every point to the major principal strain, λ_1 (Fig. 4).

CONTRACTION ACROSS SHEAR ZONE

Influence of the rate of translation $\dot{x}_T$

Assume the values of $\dot{e}_x$ and t are constant so that the intensity of pure shear outside the shear zone, given by the product, $p = \dot{e}_x t$, is constant.

For given values of $\dot{e}_x$, t and $\dot{x}_T$, Fig. 5 shows the variation across the shear zone of the major principal finite strain λ_1 and of the angle Φ_M. The value of λ_1 increases with $\dot{x}_T$ from the edges of the zone to the central part where the strain is homogeneous. The angle Φ_M reaches a maximum value (Φ_M) max; the ordinate y_M of this maximum increases with the value of $\dot{x}_T$ and is situated at a point where the intensity of λ_1 reaches a given value (λ_1) max.

Depending on the direction of variation of Φ_M, two zones can be distinguished: (i) a central zone $(0 \leqslant y \leqslant y_M)$ with prominent influence of simple shear is characterized by the increase of Φ_M to its maximum value (Φ_M) max, and is surrounded by (ii) two zones with prominent influence of pure shear $(y_M \leqslant y \leqslant h)$ where Φ_M decreases from its maximum value to zero at the boundary $(y = h)$ of the shear zone. The central zone exists only when $\dot{x}_T$ is strong enough (Fig. 5a) and its thickness increases with increasing $\dot{x}_T$. The existence of a maximum for Φ_M results in a point of inflexion on the strain trajectories (Fig. 6).

In the zone of homogeneous strain $(0 \leqslant y \leqslant h_1)$, Φ_M is constant; the curves showing its variation as a function of $\dot{x}_T$ are drawn for several values of p, t being constant (Fig. 7) and for several values of $\dot{e}_x$ and t, so that p is constant (Fig. 8). Φ_M increases from zero for $\dot{x}_T = 0$ in the case of pure shear, reaches a maximum value (Φ_M) max for $(\dot{x}_T)$ max and then decreases to very low values as $\dot{x}_T$ continues to increase. The value of (Φ_M) max depends only on the intensity of pure shear (Fig. 8) and decreases when p increases (Fig. 7) ($p = 0$ corresponds to simple shear), whereas $(\dot{x}_T)$ max depends on the values of $\dot{e}_x$ and t (Fig. 8). For a given value of $\dot{e}_x$ and t, the same angle Φ_M can be obtained from two different values $(\dot{x}_T)_1$ and $(\dot{x}_T)_2$ of the rate of translation (Fig. 7), these values being linked by the relation:

$$(\dot{x}_T)_1 (\dot{x}_T)_2 = (\dot{x}_T)^2 \text{ max}. \tag{11}$$

The shapes of the curves $\Phi_M = f(\lambda_1)$ (Fig. 9) are obviously similar to those of the curves $\Phi_M = f(\dot{x}_T)$. However, to a given value of p there corresponds only one curve $\Phi_M = f(\lambda_1)$, whatever the value of $\dot{e}_x$ and t. Therefore, for a given angle Φ_M, two λ_1 values (in general different) occur, $(\lambda_1)_1$ and $(\lambda_1)_2$, (Fig. 9) such that:

$$(\lambda_1)_1 (\lambda_1)_2 = \cot^2 \Phi_M. \tag{12}$$

If $(\lambda_1)_{cs}$ is the value linked to the simple shear ($p = 0$) for which the same angle Φ_M is obtained (Fig. 9), we have $(\lambda_1)_{cs} = \cot^2 \Phi_M$, and therefore

$$(\lambda_1)_1 (\lambda_1)_2 = (\lambda_1)_{cs}. \tag{13}$$

Therefore, for a given orientation of the principal strains, the intensity of the finite strain is always higher in the case of simple shear than in the case of simultaneous pure shear and simple shear; in the latter case, and for a given value of p, two different intensities of finite

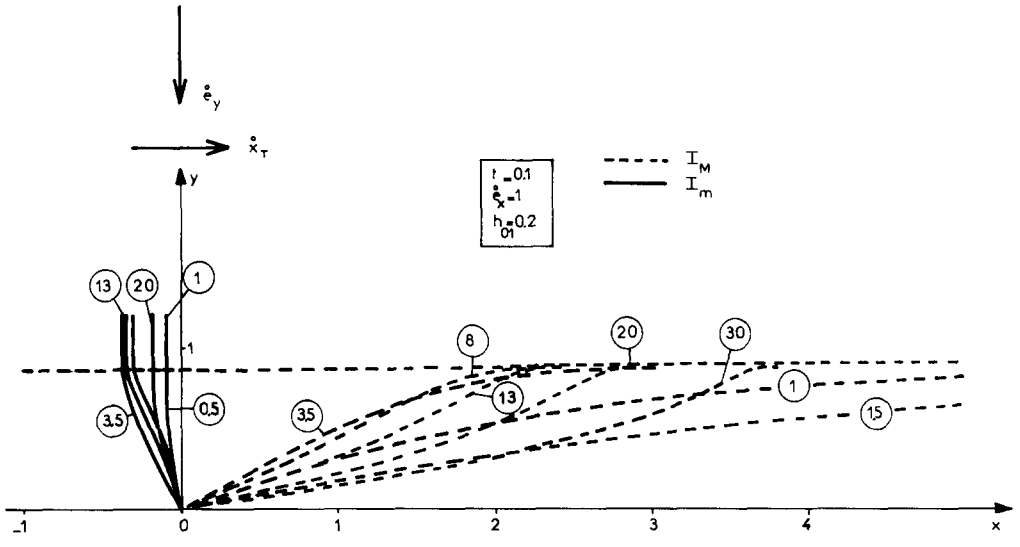

Fig. 6. Finite strain trajectories corresponding to Fig. 5 ($\dot{x}_T$ numbered).

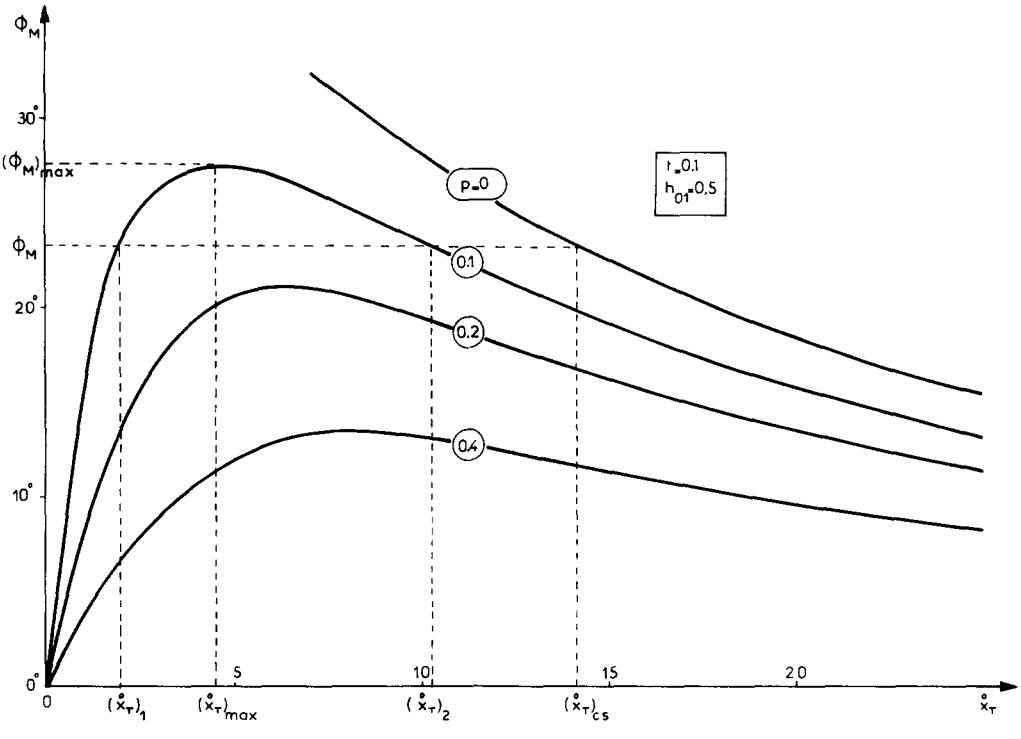

Fig. 7. Central zone with homogeneous strain: variation of Φ_M with increasing $\dot{x}_T$ for several values (numbered) of $p = \dot{e}_x t$.

strain correspond to the same orientation of the axes of the finite strain ellipse: the greater the difference between $(\lambda_1)_1$ and $(\lambda_1)_2$, the smaller the angle Φ_M and the weaker the intensity of pure shear p (Fig. 9).

When the intensity of pure shear p outside the shear zone is unknown, a double infinity of values of finite strain corresponds to each value of Φ_M.

Therefore, for a given value of p, the strain trajectories can be indeterminate in the homogeneous strain zone, although the values of $\dot{x}_T$, and thus those of the principal strains, are different; such curves, as well as those for simple shear resulting in the same angle Φ_M, are drawn in Figs. 10 and 11. In order to distinguish the two possible values of finite strain it is necessary to consider the heterogeneous strain zone: for $(\dot{x}_T)_1 < (\dot{x}_T)$ max and thus for the value $(\lambda_1)_1$ no zone of prominent influence of simple shear appears and Φ_M decreases; for $(\dot{x}_T)_2 > (\dot{x}_T)$ max and thus for the value $(\lambda_1)_2$, the zone of prominent influence of pure shear must appear; Φ_M increases, reaches its maximum value (Φ_M) max in y_M and then decreases to zero at the boundary of shear zone.

Influence of time t

Assume the value of $\dot{e}_x$ and $\dot{x}_T$ are constant and thus the intensity of pure shear (characterized by the product

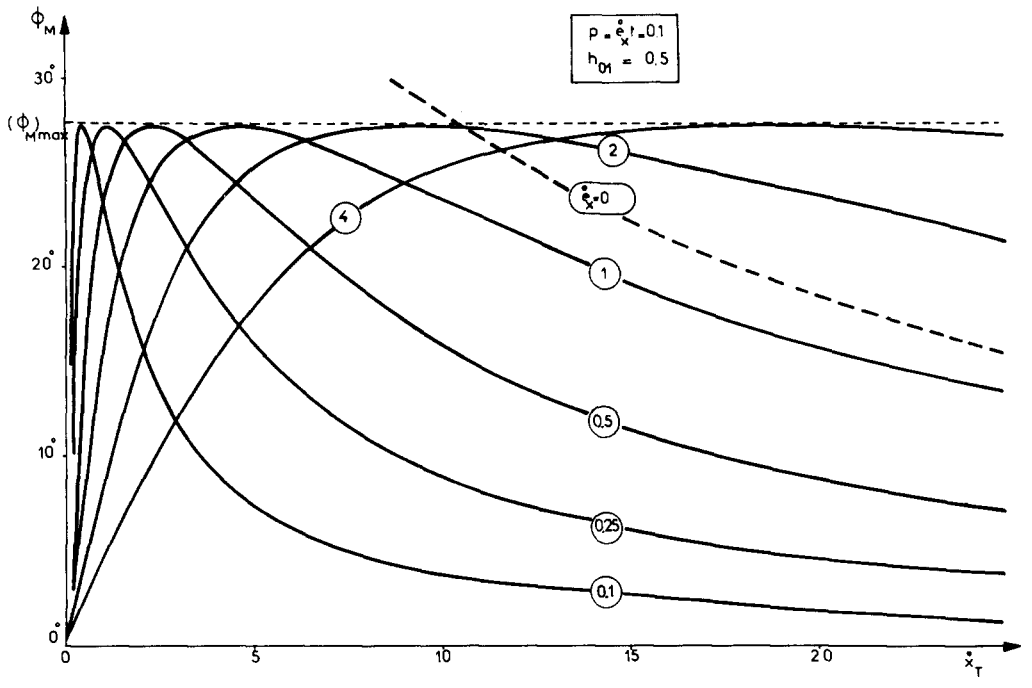

Fig. 8. Central zone with homogeneous strain: variation of Φ_M with increasing $\dot{x}_T$ for several values of $\dot{e}_x$ (numbered) and t such that $p = \dot{e}_x t$ = constant.

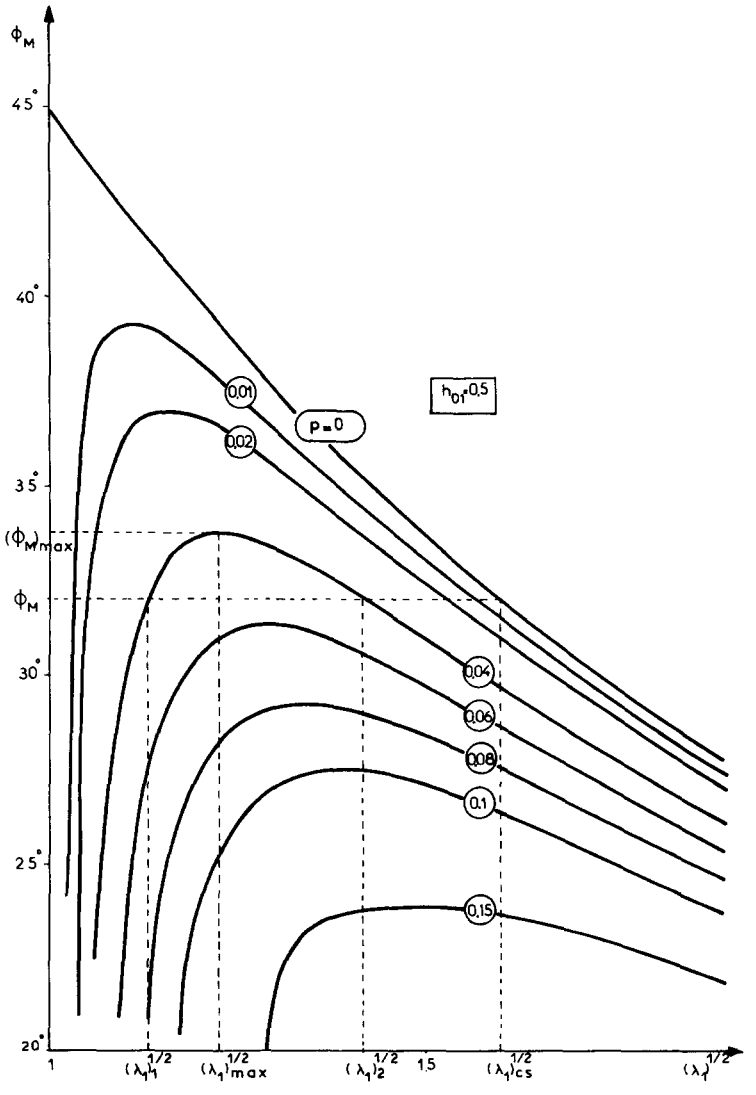

Fig. 9. Central zone of homogeneous strain: variation of Φ_M with increasing $\lambda_1^{1/2}$ for several values of p (numbered).

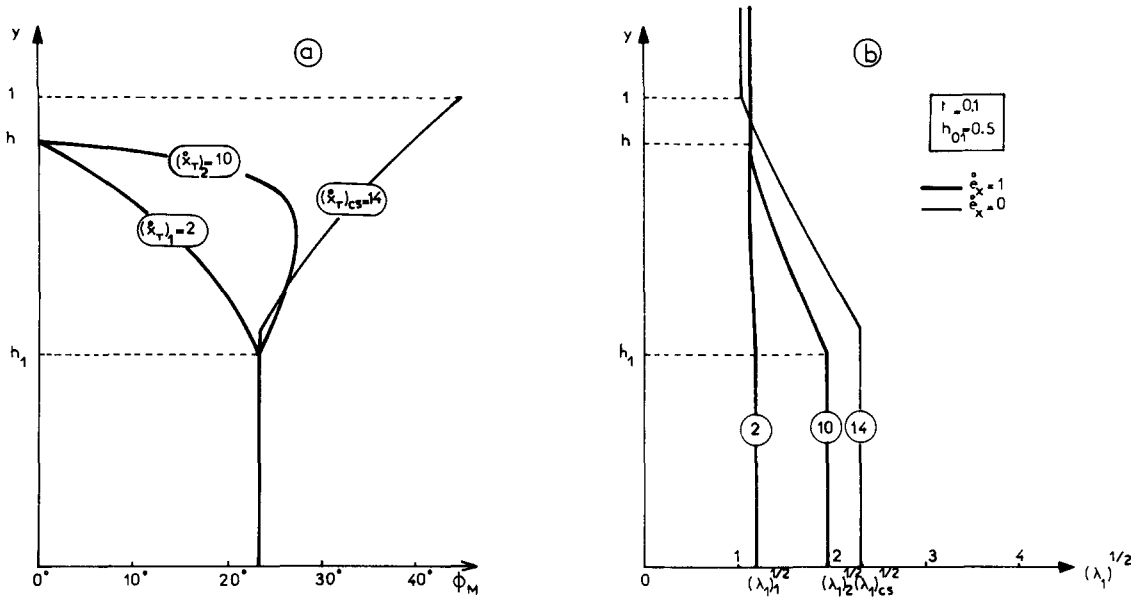

Fig. 10. Variation of (a) Φ_M and of (b) $\lambda_1^{1/2}$ throughout the shear zone: the values $(\dot{x}_T)_1 = 2$ and $(\dot{x}_T)_2 = 10$ correspond to superposition of simple shear and pure shear; the value $(\dot{x}_T)_{cs} = 14$ corresponds to simple shear alone.

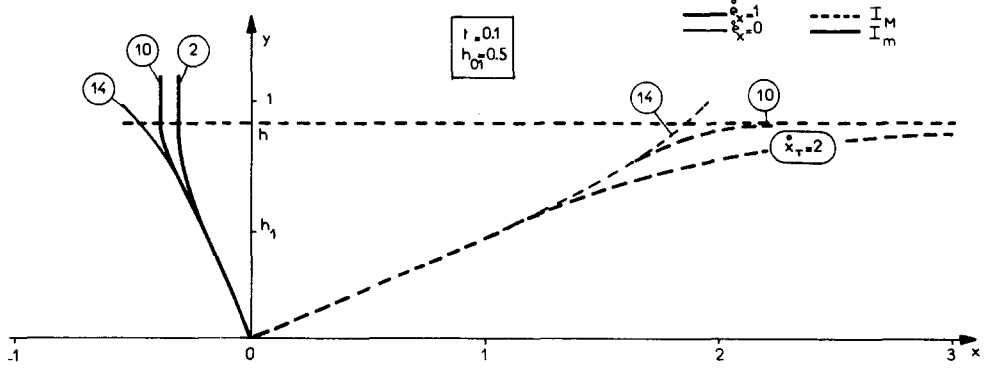

Fig. 11. Finite strain trajectories corresponding to Fig. 10.

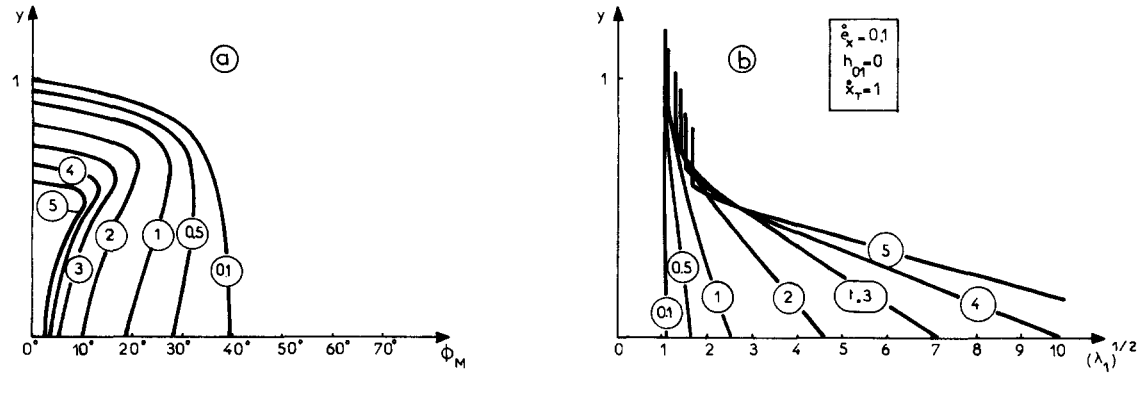

Fig. 12. Variation of (a) Φ_M and (b) $\lambda_1^{1/2}$ throughout the shear zone, for several values of t numbered.

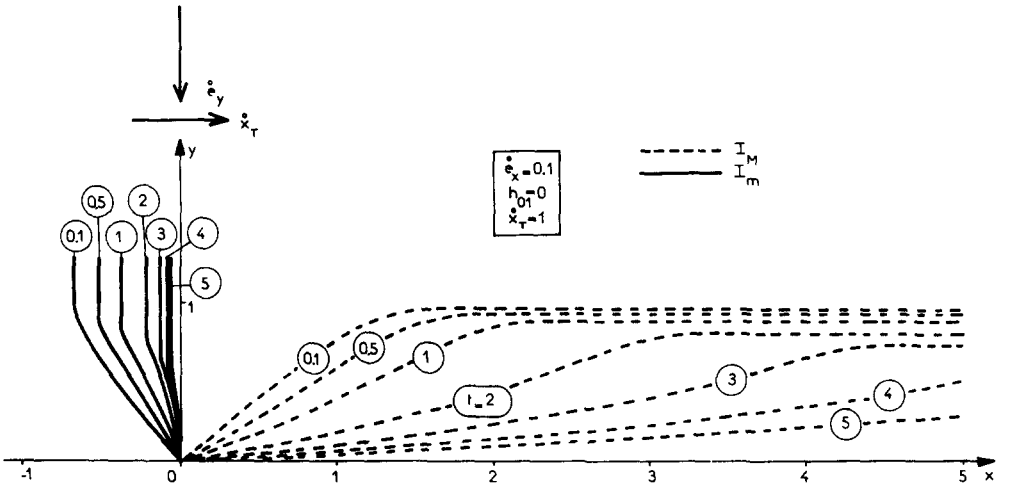

Fig. 13. Finite strain trajectories corresponding to Fig. 12.

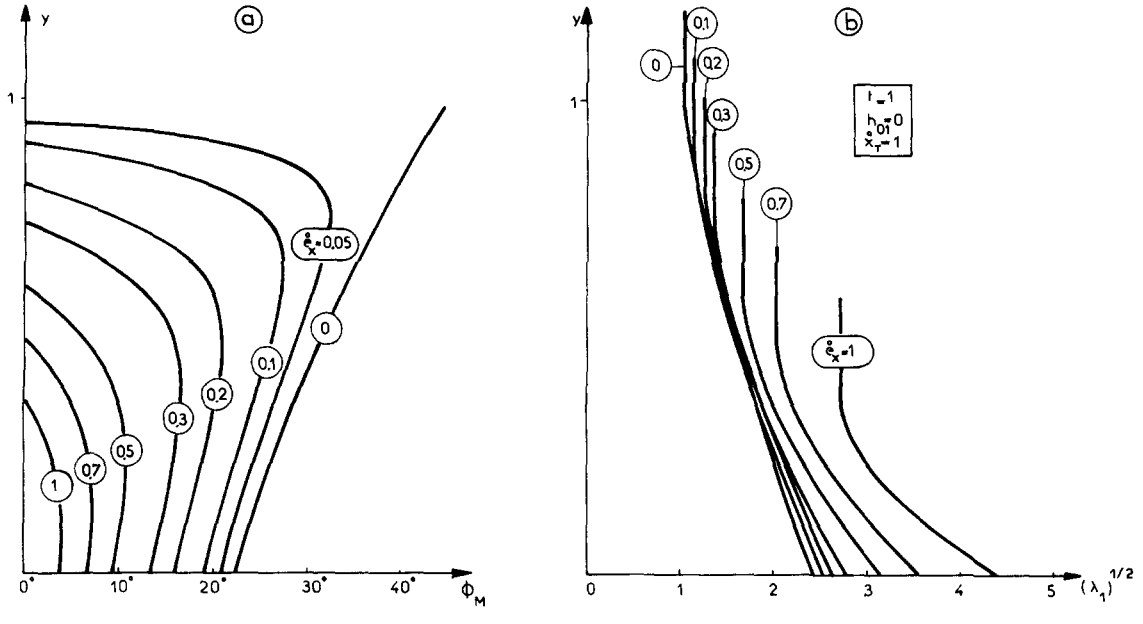

Fig. 14. Variation of (a) Φ_M and (b) $\lambda_1^{1/2}$ throughout the shear zone, for several values of $\dot{e}_x$ numbered.

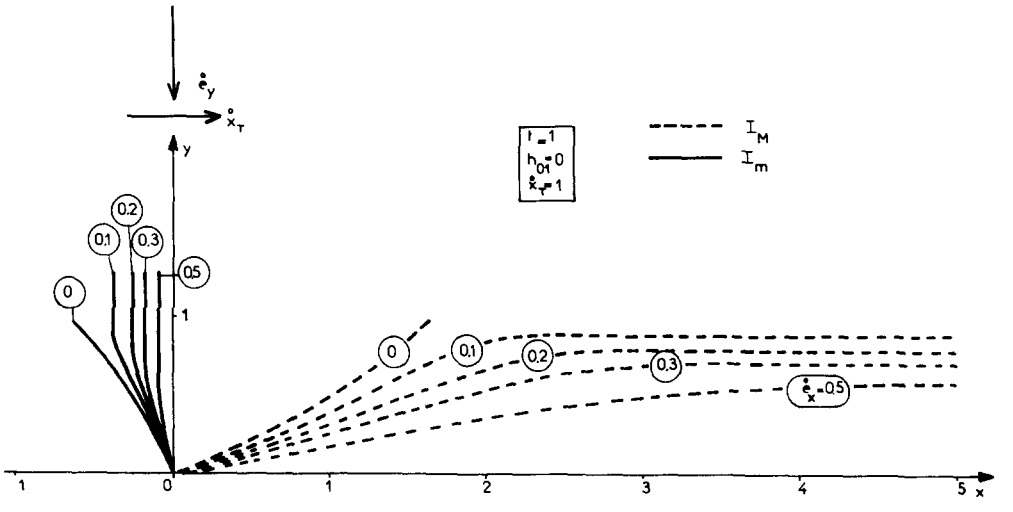

Fig. 15. Finite strain trajectories corresponding to Fig. 14.

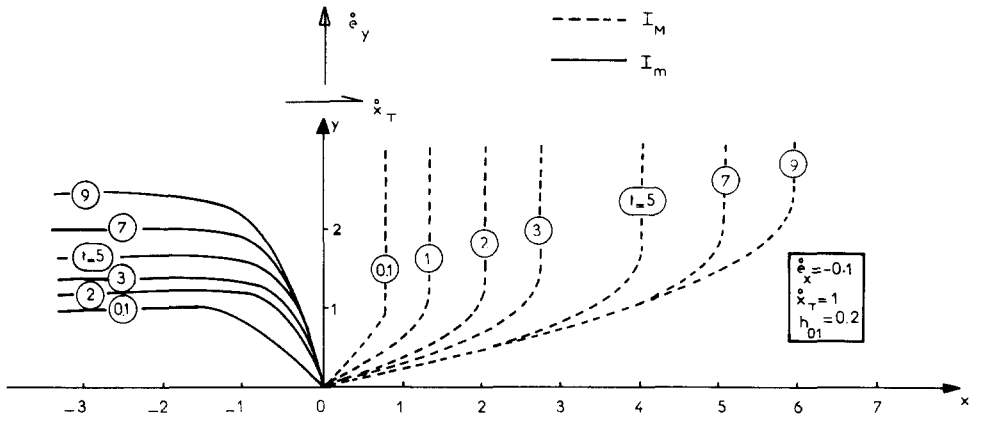

Fig. 16. Simple shear combined with extension perpendicular to the shear zone: strain trajectories for several values of t (numbered). Compare the shape of the curves I_M with that of the schistosity in Fig. 2.

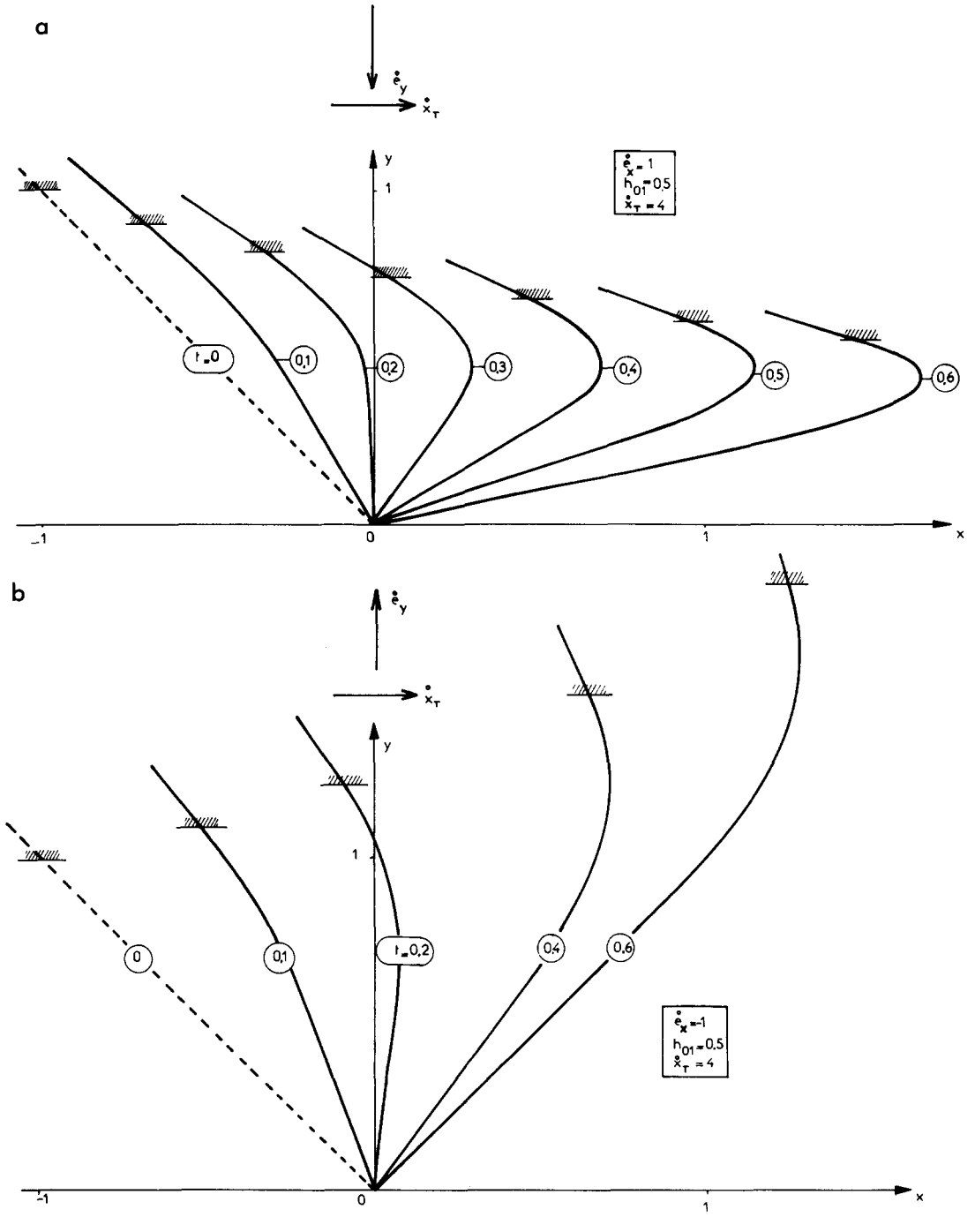

Fig. 17. Warping of initially rectilinear passive markers with increasing t (numbered) during contraction (a) perpendicular to the shear zone or (b) extension perpendicular to the shear zone.

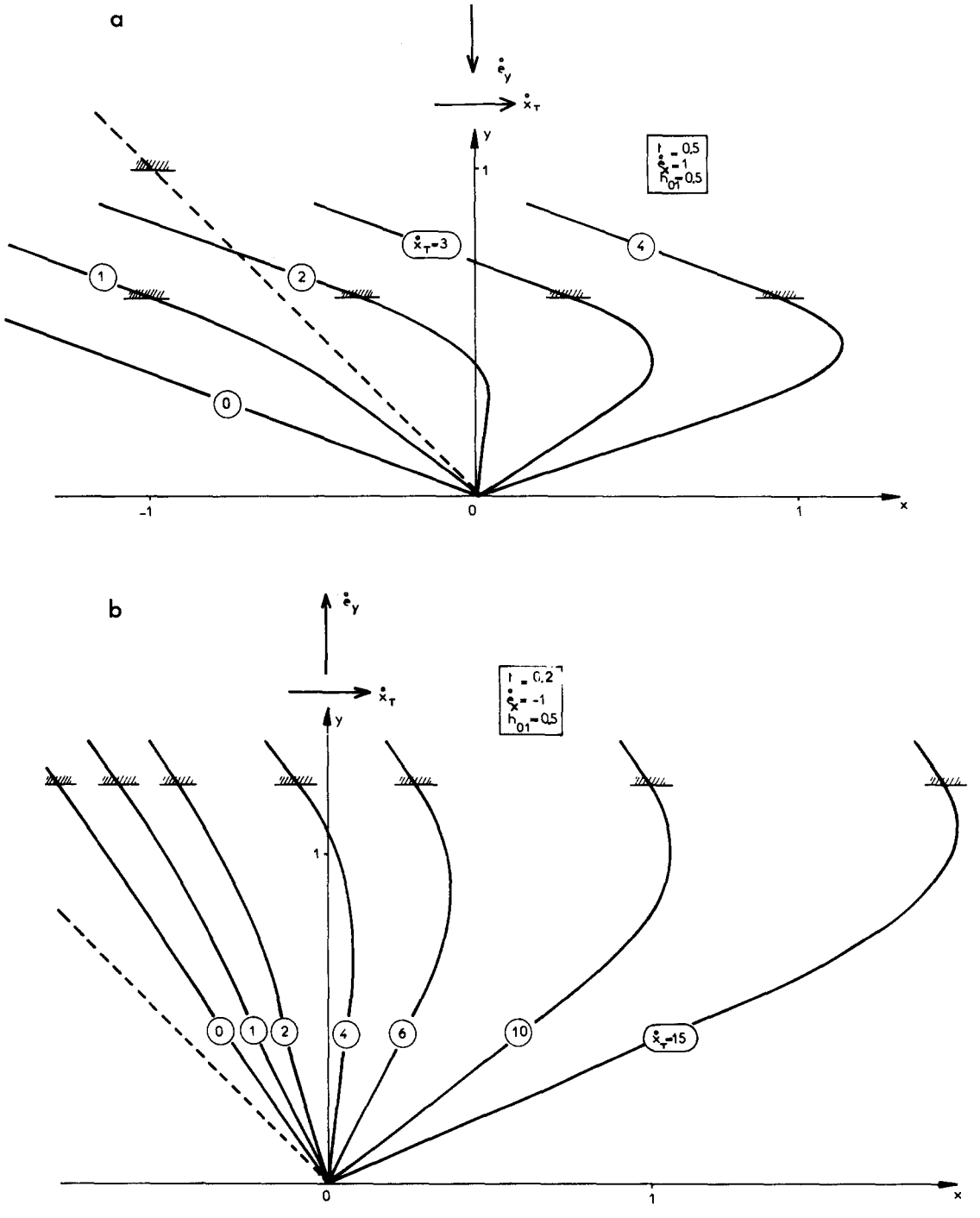

Fig. 18. Warping of initially rectilinear passive markers with increasing $\dot{x}_T$ (numbered) during contraction (a) perpendicular to the shear zone or (b) extension perpendicular to the shear zone.

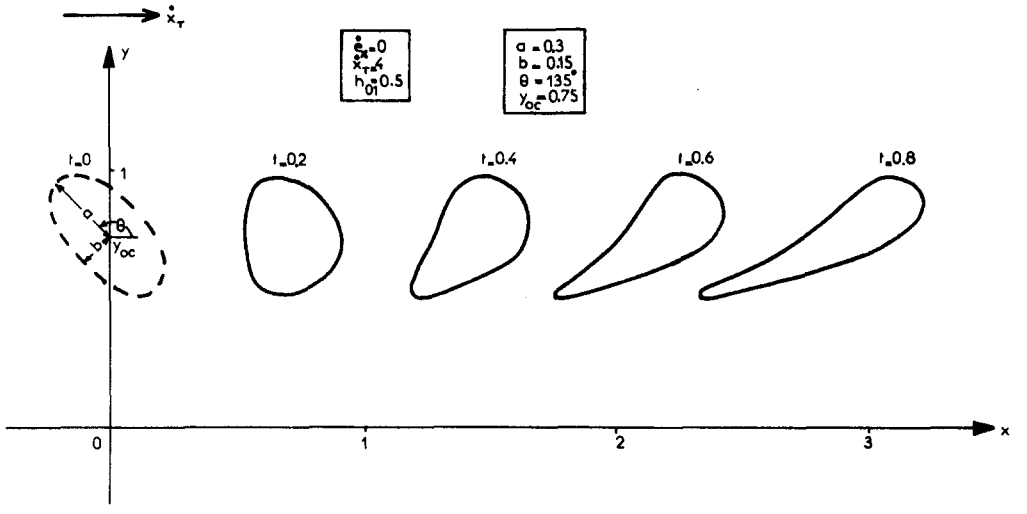

Fig. 19. Simple shear zone: evolution of initially elliptical passive markers with increasing t.

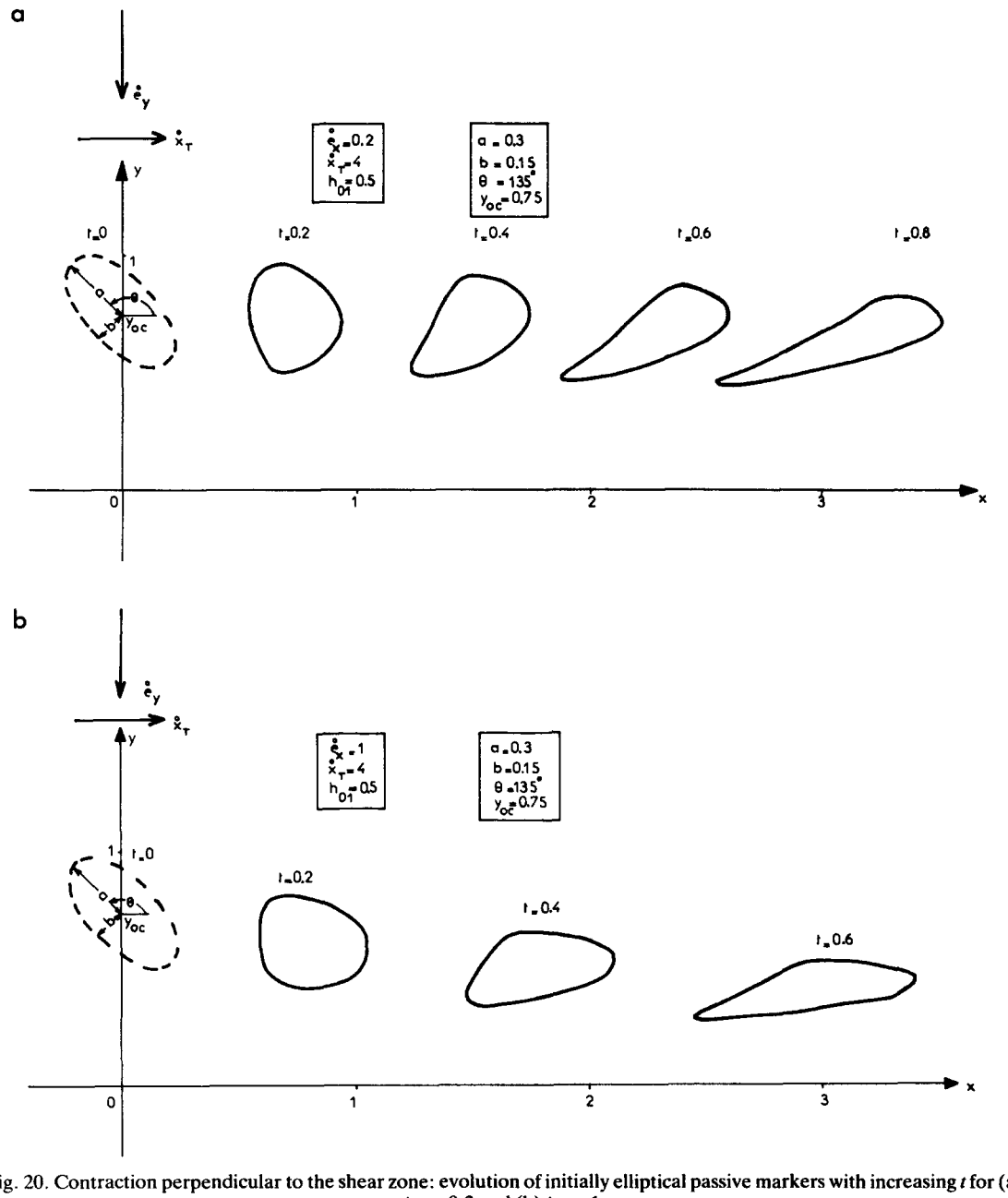

Fig. 20. Contraction perpendicular to the shear zone: evolution of initially elliptical passive markers with increasing t for (a) $\dot{e}_x = 0.2$ and (b) $\dot{e}_x = 1$.

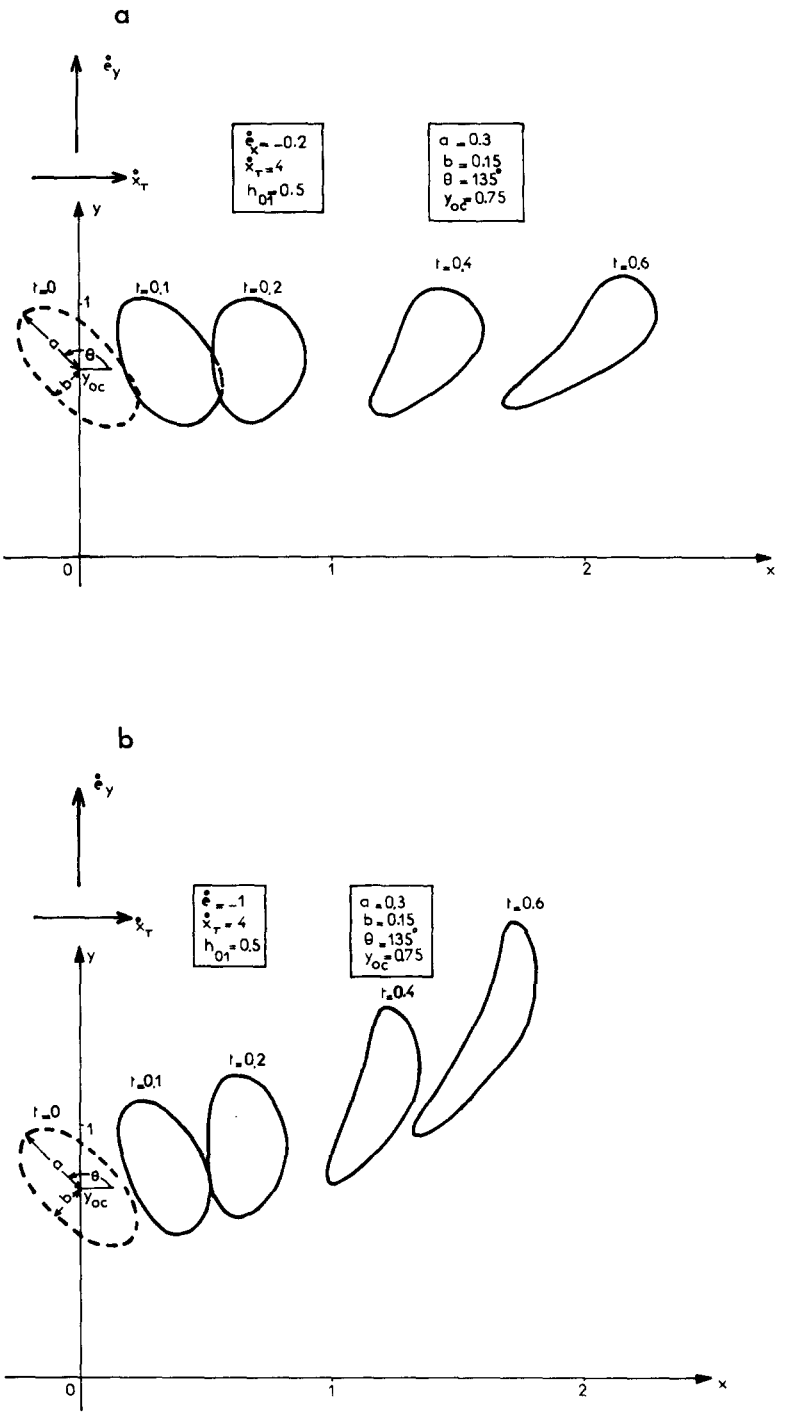

Fig. 21. Extension perpendicular to the shear zone: evolution of initially elliptical passive markers with increasing t for (a) $\dot{e}_x = -0.2$ and (b) $\dot{e}_x = -1$.

$p = \dot{e}_x t$) and that of displacement by translation of the non-sheared zone ($x_T = \dot{x}_T t$) increases with time t.

With increasing t, the values of (Φ_M) max decrease and those of (λ_1) max and of the relative thickness of the zone of dominant simple shear increase (Fig. 12); the corresponding strain trajectories are shown in Fig. 13.

Influence of the principal strain rate $\dot{e}_x$

Assume the values of t and $\dot{x}_T$ are constant and thus the intensity of pure shear increases with $\dot{e}_x$ whereas that of the displacement by translation, $(x_T = \dot{x}_T)$, is constant; the value of $\dot{\gamma}$ defined by (1 and 6) increases with $\dot{e}_x$.

Figure 14 shows that (λ_1) max increases with $\dot{e}_x$ whereas (Φ_M) max and the thickness of the zone of dominant simple shear decreases; the corresponding curves I_M and I_m are shown in Fig. 15.

The strain trajectories drawn in Fig. 16 for several values of t correspond to the case when the shear zone is simultaneously extended perpendicular to the walls; we note that the shape of the curves I_M (perpendicular at every point to the minor principal strain) agrees well with that of the natural schistosity of Fig. 2.

PASSIVE STRAIN MARKERS

Our knowledge of the particle path allows us to study the shape changes of passive strain markers with the same rheological properties as the surrounding material.

We show the change in shape of initially rectilinear passive markers with increase in t and $\dot{x}_T$ (Figs. 17 and 18) and of initially elliptical passive markers (Figs. 19, 20 and 21) in shear zones simultaneously undergoing either contraction or extension perpendicular to the walls.

CONCLUSIONS

My simple model represents the variation of the rate of shear strain $\dot{\gamma}$ throughout the shear zone.

When the shear zone simultaneously undergoes simple shear and pure shear, continuity of deformation at the boundary of the sheared material requires that $\dot{\gamma}$ be a well-defined function of time and of the rate of translation $\dot{x}_T$ of the non-sheared material.

When $\dot{x}_T$ is kept constant, we can determine the finite strain from the particle path and its evolution with time. In doing so, we can define the finite-strain trajectories which allow us to study the influence of several parameters on the formation and evolution of oriented internal structures such as the schistosity developed in ductile zones, or tension gashes in brittle-ductile zones.

This work shows the complex variation of finite strain in zones of ductile deformation where pure shear and heterogeneous simple shear act simultaneously; in general, it is very difficult to measure finite strain from the orientation of natural structures, even those sub parallel to principal strains (schistosity for example) as an infinity of strain values corresponds to each value of Φ_M.

The particle path also allows us to study the progressive shape changes of markers with the same rheological properties as the surrounding material.

Acknowledgements—The author is very grateful to Dr. P. R. Cobbold for help in improving the final version of the paper.

REFERENCES

Cobbold, P. R. 1977. Description and origin of banded deformation structures—I. Regional strain, local perturbations, and deformation bands. *Can. J. Earth Sci.* **14**, 1721–1731.

Coward, M. P. 1976. Strain within ductile shear zones. *Tectonophysics* **34**, 181–197.

Elliott, D. 1972. Deformation paths in structural geology. *Bull. geol. Soc. Am.* **83**, 2621–2638.

Gray, D. R. & Durney, D. W. 1979. Investigation on the mechanical significance of crenulation cleavage. *Tectonophysics* **58**, 35–79.

Hara, I., Takeda, K. & Kimura, T. 1973. Preferred lattice orientation of quartz in shear deformation. *J. Sci. Hiroshima Univ.* **7**, 1–11.

Jaeger, J. C. 1969. *Elasticity, Fracture and Flow*, Methuen Paperback, London, U.K.

Nadai, A. 1950. *Theory of Flow and Fracture of Solids*, McGraw-Hill, New York.

Ramberg, H. 1975. Particle paths, displacement and progressive strain applicable to rocks. *Tectonophysics* **28**, 1–37.

Ramsay, J. G. 1967. *Folding and Fracturing of Rocks*. McGraw-Hill, New York.

Ramsay, J. G. 1979. Shear zone geometry: a review. *J. Struct. Geol.* **2**, 83–99.

Ramsay, J. G. & Graham, R. H. 1970. Strain variation in shear belts. *Can. J. Earth Sci.* **7**, 786–813.

Reiner, M. 1960. *Deformation, Strain and Flow*. H. K. Lewis, London.